© 2015 IJSRSET | Volume 1 | Issue 4 | Print ISSN : 2395-1990 | Online ISSN : 2394-4099
Themed Section: Engineering and Technology

Study the Electrochemical Corrosion Behavior, Microstructure and Some Physical Properties of Lead- Calcium Rapidly Solidified Alloys

Abu Bakr El- Bediwi[*1], Sanaa Razzaq Abbas[2], Rizk Mostafa Shalaby[3], Mustafa Kamal[4]
[*1, 3, 4]Metal Physics Lab., Physics Department, Faculty of Science, Mansoura University, Egypt
[2]Ministry of Education, Iraq

ABSTRACT

Electrochemical corrosion behavior, microstructure, elastic modulus, Vickers hardness, internal friction and electrical resistivity of lead- calcium rapidly solidified alloys have been investigated. Elastic modulus of $Pb_{99.5-x}Ca_{0.5+x}$ (x=0, 0.1, 0.2, 0.3, 0.4 and 0.5 wt. %) alloys increased with increasing Ca content. Also internal friction values of $Pb_{99.5-x}Ca_{0.5+x}$ alloys variable decreased with increasing Ca content. But Vickers hardness and thermal diffusivity values of $Pb_{99.5-x}Ca_{0.5+x}$ alloys variable increased with increasing Ca content. Electrical resistivity values of $Pb_{99.5-x}Ca_{0.5+x}$ alloys decreased with increasing Ca content. The corrosion potential of Pb and $Pb_{99.5-x}Ca_{0.5+x}$ (x= 0.2 and 0.5 wt. %) alloys exhibited a negative potential. Also the cathodic and the anodic polarization curves also showed similar corrosion trends. The corrosion resistance of $Pb_{99.5-x}Ca_{0.5+x}$ alloy in 0.25 M HCl increased with increasing Ca content ratio. The $Pb_{99}Ca_1$ alloy has best properties for storage battery grids.

Key words: corrosion behavior, Vickers hardness, internal friction, elastic moduli**,** electrical resistivity**,** lead-calcium alloys

I. INTRODUCTION

Lead-calcium alloys have replaced lead-antimony alloys in a number of applications, in particular, storage battery grids and casting applications. These alloys contain 0.03 to 0.15% Ca. More recently, aluminum has been added to calcium-lead and calcium-tin-lead alloys as a stabilizer for calcium. Effects of alloying elements on structure, mechanical and electrical properties of lead-tin rapidly solidified alloys have been investigated [1-5]. Effect of adding calcium on structure, electrical, thermal and mechanical properties of lead- antimony- tin rapidly solidified alloy have investigated [6]. The measured properties of lead- antimony- tin affected after adding different ratio of calcium content. The effects of adding different ratio of calcium (0.03 to 0.13 wt. %) and tin (0.3 to 1.5 wt. %) content on microstructure, mechanical properties and corrosion resistance of Pb-Ca-Sn cast alloy have been investigated [7]. Corrosion resistance and mechanical properties of Pb-Ca-Sn alloy are found to increase with increasing tin and decreasing calcium levels.

The effect of adding Sn on the precipitation in Pb-Ca binary alloys has been studied using observations such as metallographic, hardness and resistivity measurements, and transmission electron microscopy [8]. The results show that, with increasing Sn content, the cell advance of discontinuous precipitation is retarded and continuous precipitation occurs preferentially in higher Sn content alloys. The amount of Sn necessary for the retardation is higher for higher Ca contents. The retardation effect is attributed to the segregation of Sn at advancing cell boundaries. Microstructure and electrochemical properties of lead-calcium-tin-aluminum alloys have been investigated [9]. The experimental results show that the grains gradually

became smaller as the content of calcium increased and the content of tin decreased in the alloy. The size and shape of grains were related to the ratio of tin to calcium content in the alloys. The linear sweep voltammetry and AC impedance measurements suggested that the preferred ratio of tin to calcium content is between 9 and 15 and the optimum range of tin content in the alloys is 0.8–1.1%. The properties of a Pb-Ca-Sn alloy for the positive current collector of lead-acid storage batteries, prepared by an existing industrial process and an experimental technique that involves melt jet quenching from the liquid state (GLS), have been studied [10]. The QLS process ensures good stability of the properties and structure of the alloy at elevated temperatures. Doping with trace levels of barium is shown to influence the properties of QLS ribbons. The aim of this work was to study the effects of calcium content ratio on electrochemical corrosion behavior, microstructure, Vickers hardness, internal friction, elastic moduli and electrical resistivity of lead-calcium alloys.

II. METHODS AND MATERIAL

Using high purity, more than 99.95%, lead and calcium elements, the alloys $Pb_{99.5-x}Ca_{0.5+x}$ (x=0, 0.1, 0.2, 0.3, 0.4 and 0.5 wt. %) were molten in the muffle furnace. To increase the homogeneity of the ingots the resulting ingots were turned and re-melted numerous times. From these ingots, long ribbons of about 3-5 mm width and ~ 80 μm thickness were prepared as the test samples by directing a stream of molten alloy onto the outer surface of rapidly revolving copper roller with surface velocity 31 m/s giving a cooling rate of 3.7×10^5 k/s. Using double knife cuter the samples then cut into convenient shape for the measurements. Structure of lead- calcium alloys was performed using an Shimadzu x–ray diffractometer (Dx–30, Japan) of Cu–Kα radiation with λ=1.54056 Å at 45 kV and 35 mA and Ni–filter in the angular range 2θ ranging from 20 to 100° in continuous mode with a scan speed 5 deg/min. Scanning electron microscope JEOL JSM-6510LV, Japan was used to study microstructure of lead- calcium samples. A digital Vickers micro-hardness tester, (Model-FM-7-Japan), was used to measure Vickers hardness values of lead- calcium alloys. Internal friction Q-1 and the elastic constants of lead- calcium alloys were determined using the dynamic resonance method [11-13]. Corrosion measurements of used alloys were performed using Gamry Instrument PCI4G750 Potentiostat/Galvanostat/ZRA.

III. RESULTS AND DISCUSSION

A. Microstructure

X-ray diffraction patterns of $Pb_{99.5-x}Ca_{0.5+x}$ (x=0, 0.1, 0.2, 0.3, 0.4 and 0.5 wt. %) rapidly solidified alloys show that sharp lines of face centered cubic Pb phase as offered in Figure 1. X-ray analysis such as 2θ, d Å, intensity%, FWHM, phase and hkl planes are presented in Table 1(a- f). From x-ray analysis, matrix microstructure such as lattice parameter, unit cell volume, crystal size and the shape of formed phases (such as peak intensity, peak broadness and peak position) of $Pb_{99.5}Ca_{0.5}$ alloy changed with increasing Ca content ratio. That is because Ca atoms dissolved in $Pb_{99.5}Ca_{0.5}$ matrix formed a solid solution\or and some Ca atoms formed a traces of undetected phases (Ca or Ca intermetallic phases). Calculated lattice parameter, (a), unit volume cell and crystal size values of face centered cubic Pb phase in $Pb_{99.5-x}Ca_{0.5+x}$ alloys are listed in Table 2. The results illustrated that, adding more ratio of Ca content to $Pb_{99.5}Ca_{0.5}$ alloy caused a little variation in lattice parameter and unit cell volume with a significant variation in crystal size of face centered cubic Pb phase for $Pb_{99.5}Ca_{0.5}$ alloy.

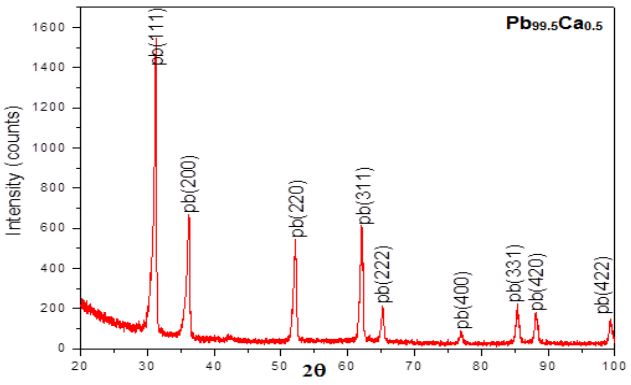

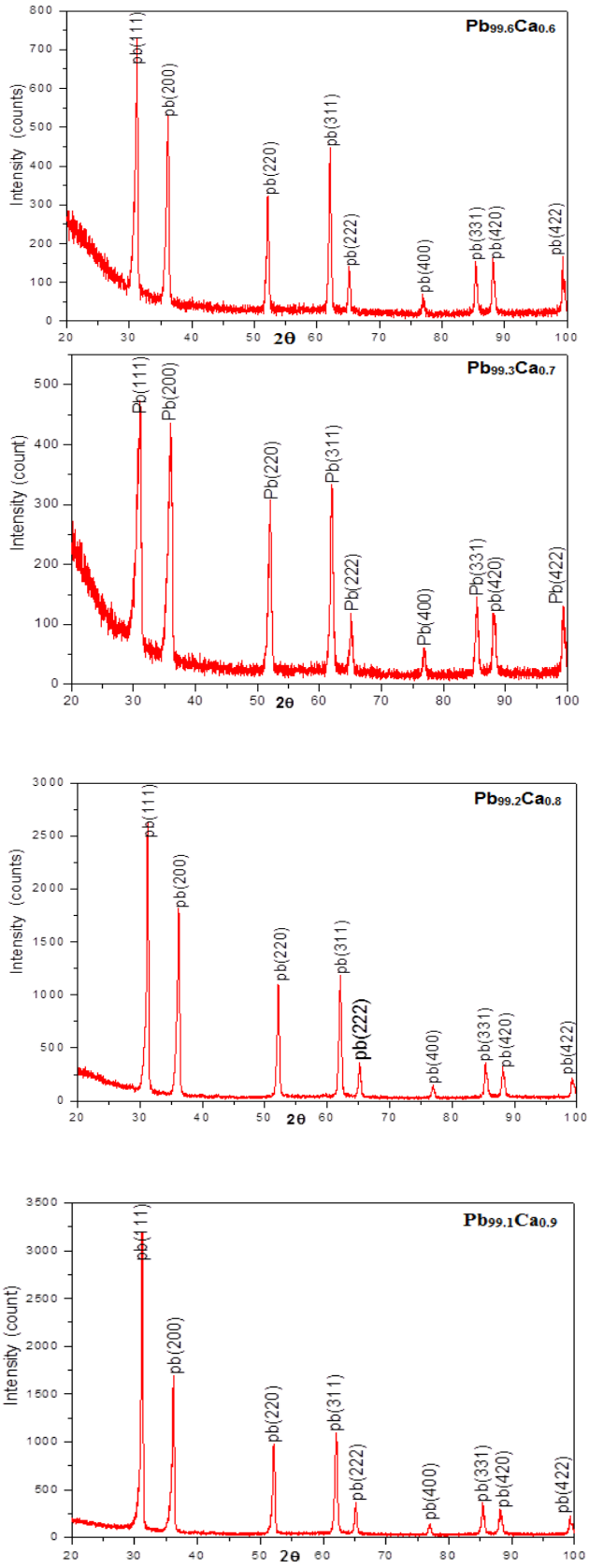

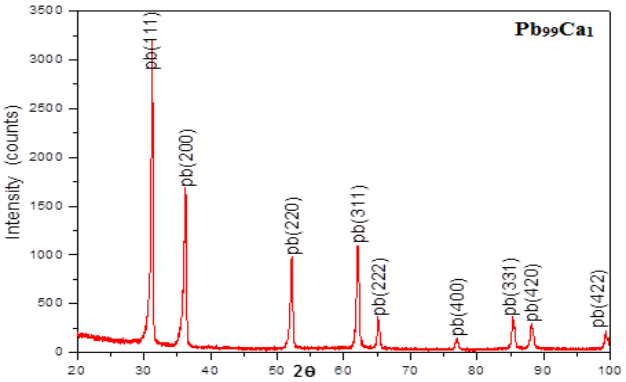

Figure 1: x-ray diffraction patterns of $Pb_{99.5-x}Ca_{0.5+x}$ alloys

Table (1a):- x-ray analysis of $Pb_{99.5}Ca_{0.5}$ alloy

2θ	d Å	Int. %	FWHM	phase	h k l
31.2378	2.86341	100	0.2362	Pb	111
36.2286	2.47959	42.57	0.2952	Pb	200
52.1796	1.75301	33.55	0.2755	Pb	220
62.0764	1.4952	39.7	0.2362	Pb	311
65.1852	1.43121	10.91	0.2362	Pb	222
76.8728	1.24016	3.67	0.2755	Pb	400
85.3554	1.13729	12.14	0.1968	Pb	331
88.0921	1.10888	9.84	0.3149	Pb	420
99.2953	1.01079	7.46	0.336	Pb	422

Table (1b):- x-ray analysis of $Pb_{99.4}Ca_{0.6}$ alloy

2θ	d Å	Int. %	FWHM	phase	h k l
31.2369	2.86349	100	0.2362	Pb	111
36.2089	2.48089	78.93	0.2952	Pb	200
52.2523	1.75074	40.32	0.3346	Pb	220
62.0441	1.4959	65.41	0.2362	Pb	311
65.2241	1.43045	16.11	0.2362	Pb	222
76.9267	1.23942	6.6	0.3936	Pb	400
85.3451	1.1374	21.13	0.1968	Pb	331
88.1059	1.10875	20.49	0.1968	Pb	420
99.2737	1.01095	12.14	0.288	Pb	422

Table (1c):- x-ray analysis of $Pb_{99.3}Ca_{0.7}$ alloy

2θ	d Å	Int. %	FWHM	phase	h k l
31.0961	2.87613	100	0.2558	Pb	111
36.0355	2.49243	97.45	0.1968	Pb	200
52.0538	1.75695	69.58	0.2165	Pb	220
62.0576	1.4956	78.72	0.1771	Pb	311
65.1214	1.43246	21.44	0.2755	Pb	222
76.9569	1.23901	9.57	0.3149	Pb	400
85.3286	1.13758	30.46	0.2362	Pb	331
88.0016	1.10979	21.17	0.2755	Pb	420
99.2906	1.01082	25.07	0.408	Pb	422

Table (1d):- x-ray analysis of $Pb_{99.2}Ca_{0.8}$ alloy

2θ	d Å	Int. %	FWHM	phase	h k l
31.2617	2.86127	100	0.2558	Pb	111
36.243	2.47864	67.3	0.2952	Pb	200
52.1744	1.75317	42.62	0.3542	Pb	220
62.0777	1.49517	44.41	0.4133	Pb	311
65.2002	1.43091	12.05	0.2362	Pb	222
76.8934	1.23987	3.78	0.2755	Pb	400
85.344	1.13741	12.09	0.2952	Pb	331
88.083	1.10898	9.34	0.2165	Pb	420
99.2971	1.01078	6.66	0.36	Pb	422

Table (1e):- x-ray analysis of $Pb_{99.1}Ca_{0.9}$ alloy

2θ	d Å	Int. %	FWHM	phase	h k l
31.2448	2.86279	100	0.2755	Pb	111
36.234	2.47923	57.72	0.2952	Pb	200
52.1463	1.75405	33.43	0.2755	Pb	220
62.1096	1.49448	33.99	0.2558	Pb	311
65.1894	1.43113	8.76	0.2165	Pb	222
76.8651	1.24026	3.12	0.1771	Pb	400
85.3108	1.13777	8.36	0.2362	Pb	331
88.1122	1.10868	7.66	0.2165	Pb	420
99.2717	1.01097	5.39	0.288	Pb	422

Table (1f):- x-ray analysis of $Pb_{99}Ca_{1}$ alloy

2θ	d Å	Int. %	FWHM	phase	h k l
31.2453	2.86274	100	0.2755	Pb	111
36.2288	2.47958	51.97	0.2952	Pb	200
52.187	1.75278	29.75	0.3346	Pb	220
62.0663	1.49542	34.16	0.3346	Pb	311
65.0808	1.43325	8.56	0.2952	Pb	222
77.0326	1.23798	3.24	0.4723	Pb	400
85.318	1.13769	9.49	0.2362	Pb	331
88.1204	1.1086	7.98	0.2362	Pb	420
99.2843	1.01087	5.02	0.24	Pb	422

Table 2:- lattice parameter, unit cell volume and crystal particle size of F.C.C Pb in $Pb_{99.5-x}Ca_{0.5+x}$ alloys

Samples	a Å	V Å^3	τ Å
$Pb_{99.5}Ca_{0.5}$	4.958	121.883	375.386
$Pb_{99.4}Ca_{0.6}$	4.944	120.812	386.988
$Pb_{99.3}Ca_{0.7}$	4.965	122.419	389.107
$Pb_{99.2}Ca_{0.8}$	4.957	121.829	340.486
$Pb_{99.1}Ca_{0.9}$	4.958	121.890	407.562
$Pb_{99}Ca_{1}$	4.958	121.867	343.857

Scanning electron micrographs, SEM, of $Pb_{99.5-x}Ca_{0.5+x}$ (x=0, 0.1, 0.2, 0.3, 0.4 and 0.5 wt. %) alloys show heterogeneous structure (same features with different orientation and size) as seen in Figure 2 and it's agreed with x-ray analysis.

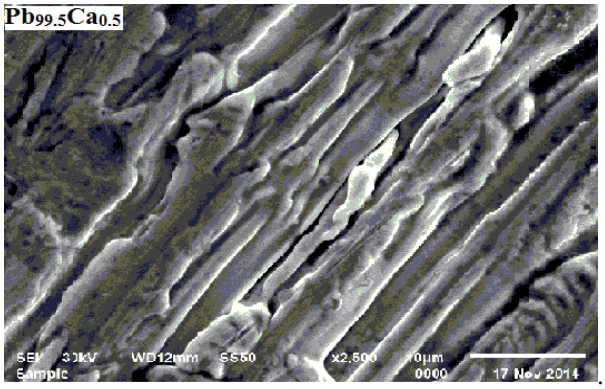

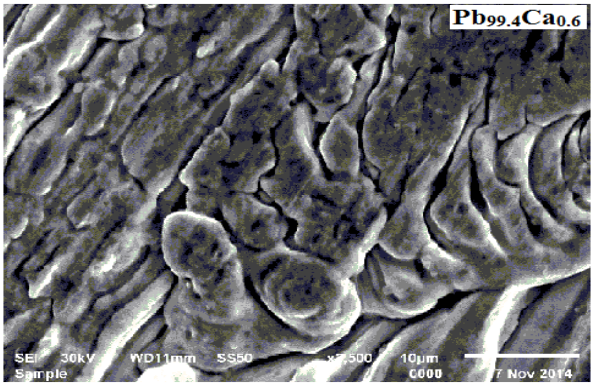

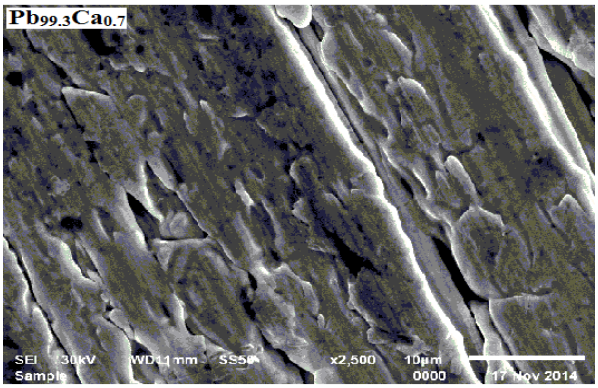

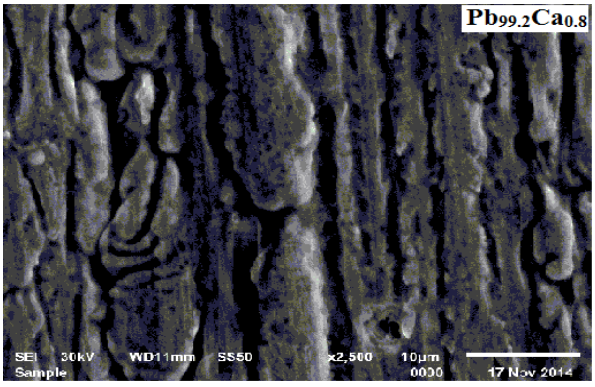

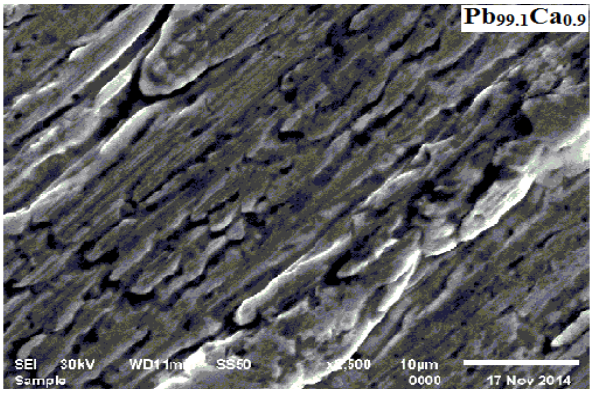

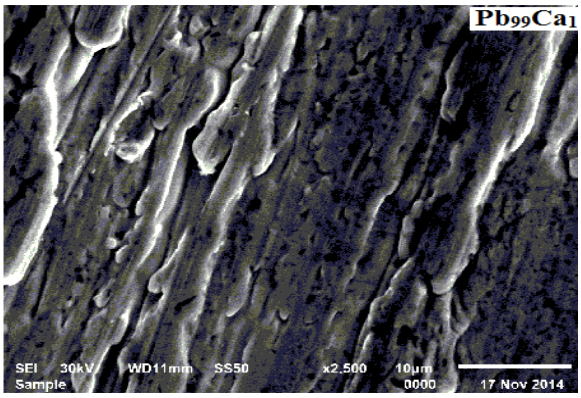

Figure 2: SEM of $Pb_{99.5-x}Ca_{0.5+x}$ alloys

B. Mechanical properties

Elastic moduli

The elastic constants are directly related to atomic bonding, structure and atomic density. The measured elastic modulus and calculated bulk modulus, B, and shear modulus, µ, of $Pb_{99.5-x}Ca_{0.5+x}$ (x=0, 0.1, 0.2, 0.3, 0.4 and 0.5 wt. %) alloys are listed in Table 3. Elastic modulus value of $Pb_{99.5}Ca_{0.5}$ alloy is increased with increasing Ca content ratio as shown in Table 5. That is because the dissolved Ca atoms formed solid solution\ or stick on grain boundary/ or formed a small cluster in $Pb_{99.5}Ca_{0.5}$ matrix, increased bond matrix strengthens.

Internal friction and thermal diffusivity

Internal friction is a useful tool for the study of structural features of alloys. Resonance curves of $Pb_{99.5-x}Ca_{0.5+x}$ (x=0, 0.1, 0.2, 0.3, 0.4 and 0.5 wt. %) alloys are shown in Figure 3 and the calculated internal friction values are presented in Table 3. Also from resonance frequency at which the peak damping occur using the dynamic resonance method the thermal diffusivity value was calculated and then listed in Table 3. The results show that, internal friction value of $Pb_{99.5}Ca_{0.5}$ alloy is variable decreased with increasing Ca content ratio.

Vickers microhardness and minimum shear stress

The hardness is the property of material, which gives it the capability to resist being enduringly deformed when a load is applied. The better of material hardness is the highest of the resistance to deformation. The Vickers hardness of $Pb_{99.5-x}Ca_{0.5+x}$ (x=0, 0.1, 0.2, 0.3, 0.4 and 0.5 wt. %) alloys at 10 gram force and indentation time 5 sec are shown in Table 4. Also calculated minimum shear stress, μ_n, of $Pb_{99.5-x}Ca_{0.5+x}$ (x=0, 0.1, 0.2, 0.3, 0.4 and 0.5 wt. %) alloys are listed in Table 4. Vickers hardness value of $Pb_{99.5}Ca_{0.5}$ alloy is variable increased with increasing Ca content ratio.

Table 3:- elastic moduli, internal friction and thermal diffusivity of $Pb_{99.5-x}Ca_{0.5+x}$ alloys

Samples	E GPa	µ GPa	B GPa	Q^{-1}	D_{th} x10^{-8} m^2/sec
$Pb_{99.5}Ca_{0.5}$	14.84±1.7	5.16	40.79	0.081	15.72
$Pb_{99.4}Ca_{0.6}$	14.91±1.7	5.18	40.88	0.072	33.08
$Pb_{99.3}Ca_{0.7}$	17.58±2	6.11	48.10	0.071	46.27
$Pb_{99.2}Ca_{0.8}$	17.97±2	6.24	49.06	0.061	56.01
$Pb_{99.1}Ca_{0.9}$	20.64±2.1	7.17	56.24	0.026	65.35
$Pb_{99}Ca_1$	20.97±2.1	7.29	57.01	0.046	40.64

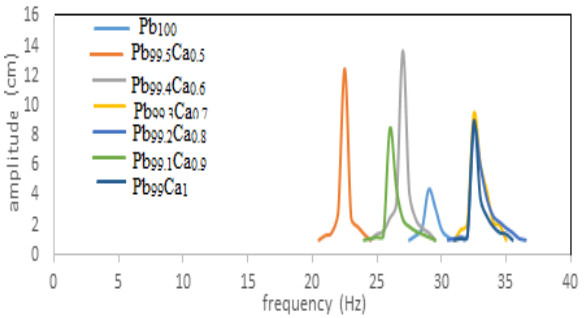

Figure 3:- resonance curves of $Pb_{99.5-x}Ca_{0.5+x}$ alloys

Table 4:- Vickers hardness and minimum shear stress of $Pb_{99.5-x}Ca_{0.5+x}$ alloys

Samples	H_v kg/mm^2	μ_n kg/mm^2
$Pb_{99.5}Ca_{0.5}$	5.25±0.75	1.73
$Pb_{99.4}Ca_{0.6}$	6.15±0.9	2.03

$Pb_{99.3}Ca_{0.7}$	5.90±0.9	1.95
$Pb_{99.2}Ca_{0.8}$	6.64±0.9	2.19
$Pb_{99.1}Ca_{0.9}$	8.05±1.1	2.66
$Pb_{99}Ca_{1}$	8.29±1.1	2.74

C. Electrical resistivity

Plastic deformation and crystalline imperfections raised electrical resistivity as a result of increasing the number of electron scattering centers. The measured electrical resistivity and calculated electrical conductivity of $Pb_{99.5-x}Ca_{0.5+x}$ (x=0, 0.1, 0.2, 0.3, 0.4 and 0.5 wt. %) alloys at room temperature using double bridge method are shown in Table 5. Electrical resistivity of $Pb_{99.5}Ca_{0.5}$ alloy decreased with increasing Ca content ratio. That is because Ca atoms dissolved in the $Pb_{99.5}Ca_{0.5}$ matrix, formed solid solution/or and some traces, decreased scattering center for conduction electrons which decreased electrical resistivity value

Table 5:- electrical resistivity and electrical conductivity of $Pb_{99.5-x}Ca_{0.5+x}$ alloys

Samples	ρ x10^{-8} Ω.m	σ x10^{6} $\Omega^{-1}.m^{-1}$
$Pb_{99.5}Ca_{0.5}$	25.58	3.91
$Pb_{99.4}Ca_{0.6}$	25.33	3.95
$Pb_{99.3}Ca_{0.7}$	21.12	4.74
$Pb_{99.2}Ca_{0.8}$	19.47	5.14
$Pb_{99.1}Ca_{0.9}$	19.22	5.21
$Pb_{99}Ca_{1}$	17.07	5.86

D. Electrochemical corrosion behavior

Electrochemical polarization curves for Pb and $Pb_{99.5-x}Ca_{0.5+x}$ (x= 0.2 and 0.5 wt. %) alloys in 0.25 M HCl are shown in Figure 4. From this figure, the corrosion potential of the Pb and $Pb_{99.5-x}Ca_{0.5+x}$ (x= 0.2 and 0.5 wt. %) alloys exhibited a negative potential. The cathodic and the anodic polarization curves also showed similar corrosion trends. Table 6 presents the corrosion potential (E_{Corr}), corrosion current (I_{Corr}), and corrosion rate (C. R) of Pb and $Pb_{99.5-x}Ca_{0.5+x}$ alloys. The results show that, the corrosion rate of $Pb_{99.5-x}Ca_{0.5+x}$ alloy in 0.25 M HCl decreased with increasing Ca content ratio. That is because increasing Ca content ratio caused a heterogeneous microstructure (changed orientation and size) which effected on microsegregation and reactivity of Ca atoms with HCl solution.

Table 6:- corrosion current, corrosion potential and corrosion rate of $Pb_{99.5-x}Ca_{0.5+x}$ alloys

Samples	I_{Corr} µA cm^{-2}	$-E_{Corr}$ mV	C. R mpy
Pb_{100}	83.90	537	101.8
$Pb_{99.3}Ca_{0.7}$	73	539	88.55
$Pb_{99}Ca_{1}$	65	538	78.82

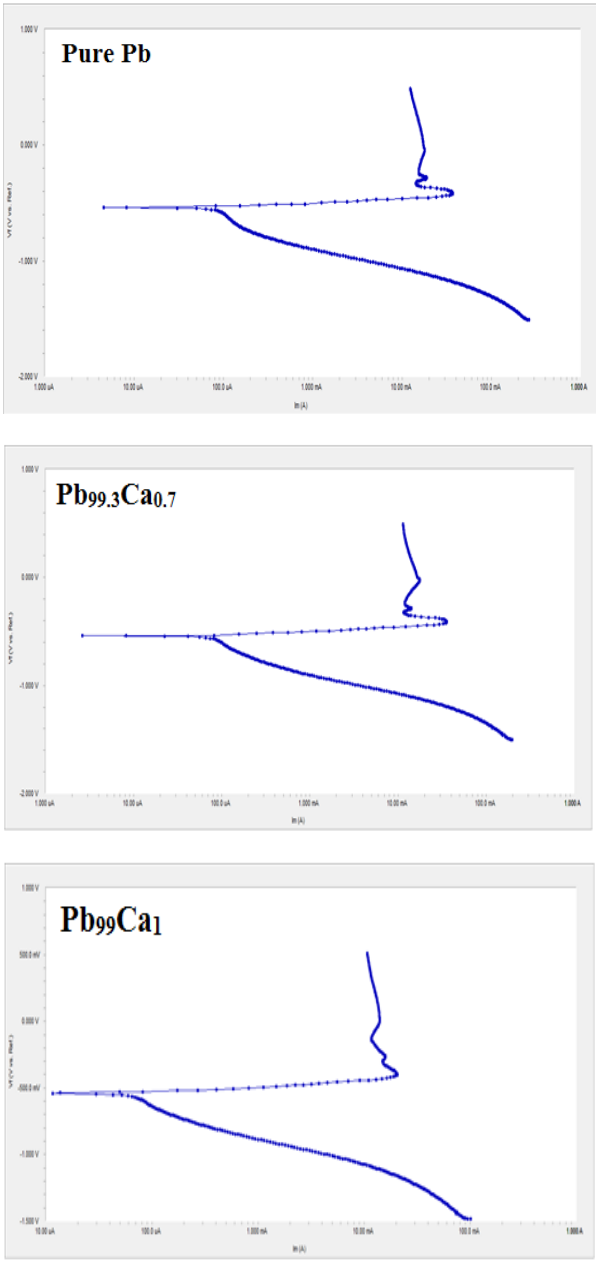

Figure 4:- electrochemical polarization curves of $Pb_{99.5-x}Ca_{0.5+x}$ alloys

IV. CONCLUSION

1. X-ray diffraction analysis show that, $Pb_{99.5-x}Ca_{0.5+x}$ (x=0, 0.1, 0.2, 0.3, 0.4 and 0.5 wt. %) rapidly solidified alloys consists of Pb face centered cubic

phase and the future of Pb phase changed with increasing Ca content ratio.

2. Elastic modulus of $Pb_{99.5-x}Ca_{0.5+x}$ (x=0, 0.1, 0.2, 0.3, 0.4 and 0.5 wt. %) alloys increased with increasing Ca content.
3. Internal friction and electrical resistivity of $Pb_{99.5-x}Ca_{0.5+x}$ alloys decreased with increasing Ca content.
4. Vickers hardness and thermal diffusivity of $Pb_{99.5-x}Ca_{0.5+x}$ alloys increased with increasing Ca content.
5. The corrosion rate of $Pb_{99.5-x}Ca_{0.5+x}$ alloy in 0.25 M HCl decreased with increasing Ca content ratio.
6. The $Pb_{99}Ca_1$ alloy has the best properties such as high strength and corrosion resistance for storage battery grids industrial

V. REFERENCES

[1] A. B. El- Bediwi. 2002. AMSE, 75: 3 (2002) 1-12

[2] M. Kamal and A. B. El-Bediwi. 2000. J. Mater. Sci. Mater. Electron. 11 (2000) 519-523

[3] M. Kamal, A. B. El-Bediwi and M. B. Karman. 1998. J. Mater. Sci. Mater. Electron. 9 (1998) 425-428

[4] M. Kamal, S. Mazan, A. B. El-Bediwi and M. El-Naggar. 2002. Radiat. Eff. Def. Sol. 157 (2002) 467-474

[5] A. B. El-Bediwi. 2005. Cryst. Res. Technol. 40: 7 (2005) 688-691

[6] M. Kamal, A. B. El-Bediwi and M. S. Jomaan. 2014. International Journal of Modern Applied Physics, (Nov2014)

[7] C.S. Lakshmi, J.E. Manders, D.M. Rice. 1998. Structure and properties of lead–calcium–tin alloys for battery grids, Journal of Power Sources, 73: 1 (18 May 1998) 23-29

[8] H. Tsubakino, M. Tagami, S. Ioku, A. Yamamoto. 1996. Precipitation in lead-calcium alloys containing tin, Metallurgical and Materials Transactions A, 27: 6 (June 1996) 1675-1682

[9] H. Li, W. X. Guo, H.Y. Chen, D. E. Finlow, H. W. Zhou, C. L. Dou, G. M. Xiao, S. G. Peng, W. W. Wei, H. Wang. 2008. Study on the microstructure and electrochemical properties of lead–calcium–tin–aluminum alloys, Journal of Power Sources 10 (2008) 59

[10] V. A. Dzenzerskii, V. F. Bashev, S. V. Tarasov, V. A. Ivanov, A. A. Kostina, S. V. Korpach. 2014. Structure and properties of a Pb-Ca-Sn battery alloy crystallized under nonequilibrium conditions, Inorganic Materials, 50: 2 (February 2014) 140-144

[11] B. D Cullity, "Element of x-ray diffraction" Ch.10 (1959) 297

[12] Sppinert S and Teffit W. E, ASTM, Proc. 61 (1961) 1221

[13] Schreiber E, Anderson O. L and Soga N, Elastic Constants and their Measurement, McGraw-Hill Book Company, Ch. 4 (1973)